IOP Conf. Series: Materials Science and Engineering **1344** (2026) 012083 doi:10.1088/1757-899X/1344/1/012083

Conceptual design of a replacement 2.1 K cold box for the Spallation Neutron Source Central Helium Liquefier

B Mastracci[1], R Bhattacharya[1], C Butler[1], J Creel[1], R Maekawa[2], M Howell[2], A Coleman[2], J Magnin[1], R Norton[1] and T Wijeratne[1]

[1] Thomas Jefferson National Accelerator Facility, Newport News, USA
[2] Oak Ridge National Laboratory, Oak Ridge, USA

*E-mail: brianm@jlab.org

Abstract. After more than 20 years of operation, the cold compressor technology in use at the Spallation Neutron Source (SNS) is obsolete, and replacement parts and service are no longer available. SNS has partnered with Jefferson Lab to design and construct a replacement sub-atmospheric cold box outfitted with modern cold compressor technology. The general design follows from Jefferson Lab's experience on other recent sub-atmospheric cold box projects. Design decisions are backed by thorough engineering analysis to ensure technical requirements are met in a cost-effective manner. Conceptual design of the replacement cold box has been completed, and will be summarized in this paper. It features five cold compressors with an operating flow range of 80-140 g/s, and includes piping and valving to support cold compressor maintenance without interrupting flow circulation to the load. The approach to thermal shielding, insulation, and integration of the upgraded cold compressor hardware into the existing SNS control system will also be addressed.

1. Introduction

The Spallation Neutron Source (SNS) at Oak Ridge National Laboratory (ORNL) is a neutron science facility driven by a linear accelerator (LINAC), part of which is a superconducting LINAC (SCL). Saturated liquid helium at 2.1 K, generated by a central helium liquefier (CHL), is used to cool the SCL.

The CHL is the result of a partnership between SNS and Thomas Jefferson National Accelerator Facility (Jefferson Lab) [1]. Its main compressor system includes six oil-flooded screw compressors and the associated oil removal system. A main or 4.5 K cold box contains the heat exchangers (some of which function as an 80 K liquid nitrogen (LN_2) precooler), turboexpanders, and cold piping required to generate liquid at 4.5 K. Sub-atmospheric saturation conditions in the SCL are achieved by a string of four cryogenic centrifugal (cold) compressors, which are located in a separate sub-atmospheric or 2.1 K cold box.

The cold compressors have been in use for about 20 years [2] and are now obsolete. They are analog active magnetic bearing (AMB) machines with LN_2 cooled motors, and are completely enclosed within the 2.1 K cold box vacuum shell. Access for repair or replacement is difficult and time consuming, and parts and service are no longer available from the manufacturer, making them an operability risk to SNS.

IOP Conf. Series: Materials Science and Engineering **1344** (2026) 012083 doi:10.1088/1757-899X/1344/1/012083

Recently constructed sub-atmospheric cold boxes use a new style cold compressor system, which features digital AMB control and an externally mounted, water cooled motor that can be serviced or replaced without breaking insulating vacuum [3,4]. SNS has again partnered with Jefferson Lab to design and build a replacement 2.1 K cold box using this newer technology. This paper will review the conceptual design details, focusing on engineering decisions that impact the general architecture of the new cold box. Section 2 covers the process design basis which leads to the general sizing and layout covered in Section 3. The approach to actively cooled shielding and multilayer insulation (MLI) configuration differ somewhat from previous designs, and will be addressed in Section 4 and Section 5, respectively. Section 6 provides a general overview of the control system, and a summary appears in Section 7.

2. Process Requirements

Three basic operating configurations guide the design and selection of components. The primary and most used configuration is for normal 2.1 K operations, and can be further divided into four operating modes: nominal, minimum, and maximum steady-state flow, and pumpdown, which is the process of reducing SCL pressure from nominally ambient to the steady-state operating value by increasing cold compressor rotational speeds. Process conditions for each mode are summarized in Table 1.

The current system at SNS typically operates at 105 g/s, so this was selected as the nominal flow rate for the new system. The maximum flow rate of 140 g/s was selected to match the observed capability of the existing system [5], and the minimum flow rate of 80 g/s was specifically requested by SNS. Flow at the start of pumpdown is adopted from the main cold box design temperature-entropy (T-S) diagram, which allows for 160 g/s and should result in a faster pumpdown than the current starting rate of 140 g/s.

The normal operating saturation pressure in the SCL is 42.6 mbar, as measured at the inlet to the 2.1 K cold box, and frictional losses and valves in the piping leading to the first cold compressor are accounted for in the suction pressure specifications. Discharge pressure specifications are based on observations of the existing cryogenic system during normal operation. Suction temperature is estimated using a basic model capturing the thermal and hydraulic performance of the SNS cryogenic distribution system. Specifying an outlet temperature

Table 1. Cold compressor process conditions for each required 2.1 K operating mode, including minimum, nominal, and maximum steady-state flow rates and pumpdown.

Mode	Mass Flow Rate	Pressure		Temperature	
		Suction[a]	Discharge	Suction	Discharge
Minimum	80 g/s	41.5 mbar	1.25 bar	4.02 K	< 30 K
Nominal	105 g/s	40.5 mbar	1.25 bar	3.84 K	< 30 K
Maximum	140 g/s	39.5 mbar	1.25 bar	3.70 K	< 30 K
Pumpdown Start	160 g/s	1.20 bar	1.20 bar	4.5 K	4.5 K

[a]Cold compressor suction pressures are based on a constant 2.1 K cold box inlet pressure of 0.042 atm.

of <30 K is common practice, though Jefferson Lab's own recently commissioned subatmospheric cold box is far more efficient [6], and it is assumed that the SNS cold box will perform similarly.

A request for information (RFI) was distributed among potential cold compressor vendors to evaluate the feasibility of the process requirements and obtain preliminary geometric and utility information. Based on the results, the new 2.1 K cold box will use five cold compressors instead of four. Since performance data was not requested, conceptual design proceeded under the assumption that each stage has an equal pressure ratio and isentropic efficiency of 75%.

The other two configurations include a backfill mode, for which a valve is provided to repressurize the SCL using 4.5 K vapor from a liquid helium storage dewar, and a bypass mode, for which a valve is provided to bypass the cold compressor train. The latter is used to operate the SCL at 4.5 K when needed. Cold compressor maintenance or replacement will also be performed in this configuration. A pair of isolation valves is provided at both the discharge and suction ends of the train to isolate it from the cold 4.5 K return path, and utilities are provided to evacuate or pressurize the space between each pair of valves with clean gas to enhance isolation. The basic process flow diagram for the new cold box, showing the cold compressors and valves required to meet the three operating configurations, is shown in Figure 1.

3. Component Sizing and Layout

Pipe running through the cold compressor train constitutes most of the equipment internal to the cold box. It is designed for minimal pressure drop as well as cold compressor stability, which is achieved with suitably large turnover time constants and by placing flow straighteners at each cold compressor inlet [7]. The time constant τ describes the amount of time required for a cold compressor to process the volume of fluid contained in its inlet piping. For this system, a target of $\tau = 0.5$ s at the maximum flow rate has been selected, and a minimum length for each potential nominal pipe size (NPS) has been computed accordingly. Each run will be u-shaped, so this length must be at least twice that required for the flow straightener (the recommendation of nine inside diameters for a differential producing flow element [8] is used as a conservative estimate). Minimum required pipe lengths are increased if necessary to meet this criterion, and then used together with known inside diameters for Schedule 10S stainless steel pipe to predict pressure drop. The smallest pipe size satisfying both $\Delta P \leq 2$ mbar and $\Delta P/P \leq 1\%$ is selected.

All components and interconnecting piping fit appropriately into a vacuum shell measuring 10 ft. in diameter by 13 ft. tall. A general arrangement is shown in the left panel of Figure 2, with

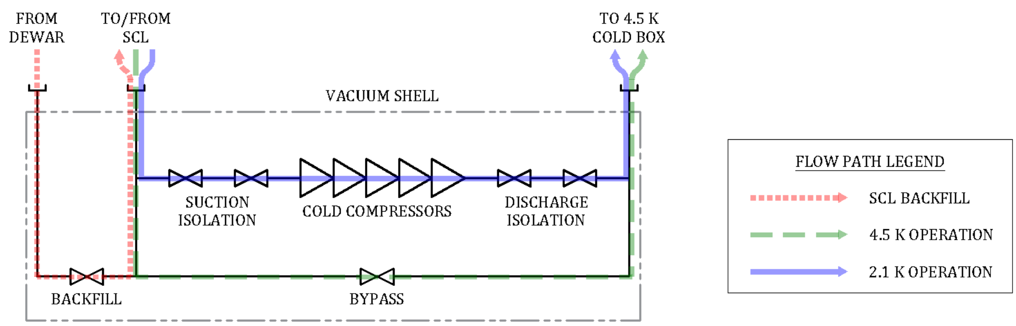

Figure 1. Basic process flow diagram for the new SNS 2.1 K cold box showing equipment and flow paths for the three required configurations: 2.1 K operations, 4.5 K operations (which includes cold compressor replacement), and SCL backfill.

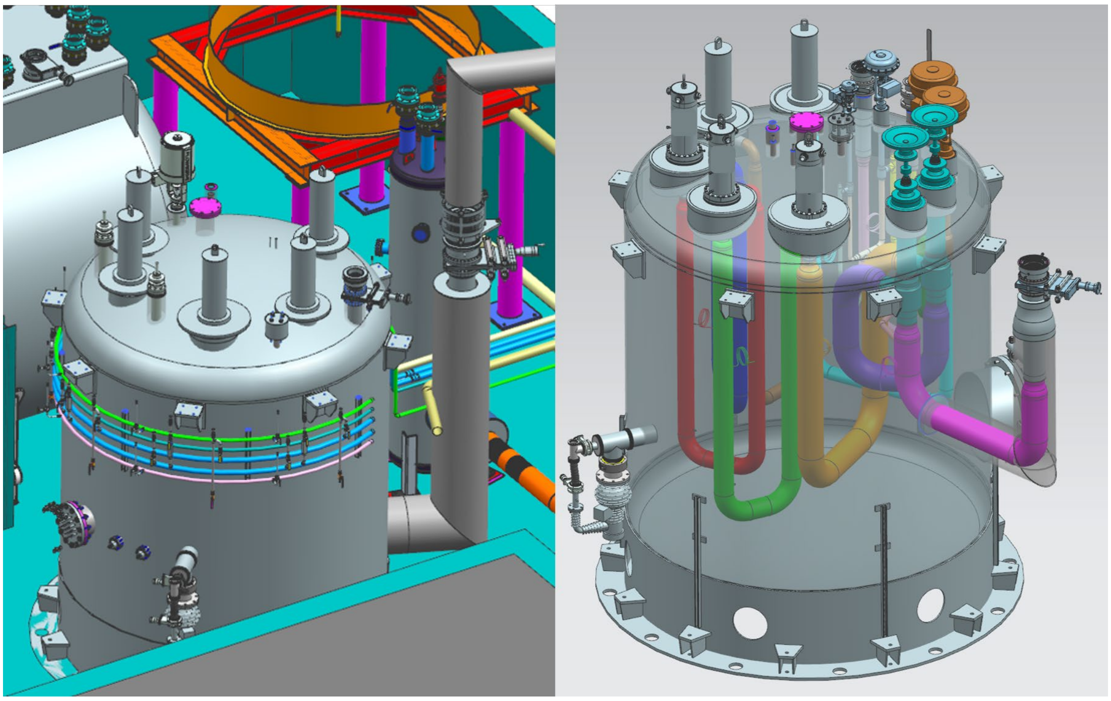

Figure 2. Left: Model of the conceptual arrangement for the new SNS 2.1 K cold box. Right: More mature model with the cold box isolated, showing the internal component layout.

internal piping visible in the right panel. Following the approach taken for Jefferson Lab's own subatmospheric cold box replacement [4], torispherical formed heads are selected for both top and bottom of the shell to reduce cost and weight associated with the flat top heads that were used previously [3,9]. Cold compressors, valves, and other equipment residing on the top head will be attached to short nozzles to compensate for curvature of the crown. All penetrations will be located on the top head to simplify the fabrication process, except that the primary return bayonet penetration will be located on the side, placing it as close as possible to the corresponding transfer line bayonet and minimizing the size and weight of the interconnecting u-tube.

Mechanical utilities and instrumentation required to support operation and maintenance of the cold compressors are located on the side of the shell. These include cooling water, guard vacuum, 4 atm helium gas, and instrument air for the control valves. Most of the utility piping was sized to match the existing installation, but the water piping size has increased due to the addition of water cooled cold compressor motors. Using the maximum motor power and allowable temperature rise estimates from the RFI, together with the existing insulating vacuum diffusion pump specifications, a maximum water flow rate was determined and used to sized the main cooling water supply and return piping such that the pressure drop is no more than 0.1 atm each.

4. Actively Cooled Shielding

Shielding the internal components of the 2.1 K cold box reduces heat absorbed by the process at low temperature, effectively reducing the primary load and lowering the power and LN_2 consumed by the warm compressors and main cold box, respectively, at the expense of the LN_2 used to cool the shield. The same applies for anchoring heat intercepts on bayonets and valve stems at 80 K. Since electricity at SNS is billed at a flat rate but LN_2 is billed per gallon, the end user has requested that minimizing LN_2 consumption take precedence over minimizing electrical power usage. A parametric study of various heat shield and thermal intercept combinations has been conducted in order to determine which configuration results in the lowest combined LN_2 usage between the main and sub-atmospheric cold boxes.

Four configurations were considered: full shielding, with all valve stems and bayonets anchored to the shield; partial shielding, up to the first cold compressor inlet only, with all thermal intercepts utilized; no shielding, but all thermal intercepts utilized; and no shielding or thermal intercepts at all. Since suction isolation valve C_v and stem heat leak will also affect the load on the 4.5 K system, three different commercially available products (referred to here only as valves "A", "B", and "C") were considered in this process so that the most advantageous combination of shielding and valves can be selected.

For each configuration, total heat absorbed by LN_2 in the 2.1 K cold box was determined and converted into a 2.1 K cold box LN_2 usage rate. The 4.5 K cold box LN_2 usage rate is deduced from the total exergetic load on the system, where the primary load consists of the combined SCL and 2.1 K cold box, and the other loads (shield, 4.5 K refrigeration, and 4.5 K liquefaction) are assumed constant at the original design conditions. The primary load exergy usage rate will depend on heat leak into the 2.1 K cold box process piping, which varies with each valve and shielding configuration. Conventional practice at Jefferson Lab is to use a conservative estimate of 4 W/m^2 for unshielded piping and 0.15 W/m^2 for shielded piping. Based on the conceptual geometry this equates to roughly 150 W for the completely unshielded case (with some minor variation among the different valve options), and may be reduced to 130 W if thermal anchors are used, 105 W if a partial shield is applied, and only 30 W in the fully shielded case. In the worst-case scenario, the heat leak penalty incurred by reducing shield coverage is less than 1% of the heat of compression, and therefore makes only a small contribution to the primary load.

The left panel in Figure 3 shows the estimated total LN_2 usage rates for each configuration, relative to that of the original design operating point. Each option offers a substantial improvement in LN_2 usage due to the anticipated superior efficiency of the new cold compressors. The lowest usage rate estimates are obtained for the unshielded and unintercepted case, provided that the suction isolation valves have a larger C_v to static heat leak ratio ("A" and "C"). As seen in

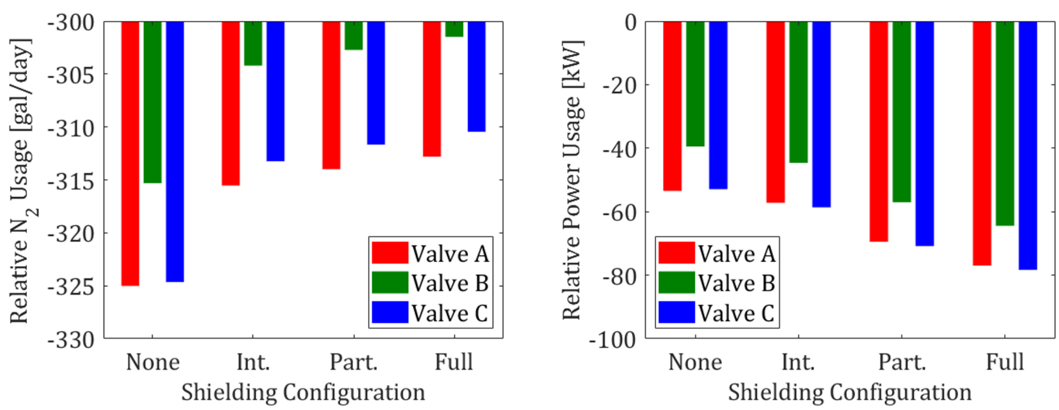

Figure 3. LN_2 and electrical power usage rates for different valves and configurations including no shield or heat intercepts (none), heat intercepts only (int.), partially shielded with heat intercepts (part.), and fully shielded with heat intercepts (full), relative to the original design usage rate.

the right panel of Figure 3, this configuration should also require less electrical power than the original design case, due again to the assumed cold compressor efficiency, though the reduction is not as large as some of the shielded configurations offer. Even without shielding, static heat leak in the 2.1 K cold box makes only a small contribution to the primary load, and eliminating LN_2 usage offers the lowest capital and operating expenditures for this particular installment.

5. Thermal Insulation

Many cold box vacuum shells at Jefferson Lab have multilayer insulation (MLI) applied to the inside surface, including the recently built replacement sub-atmospheric cold box [4]. Due to design challenges, fabrication effort, and material quantities required to insulate the shell, this practice was reviewed to ensure that insulation will be utilized in the most effective and economical manner for the SNS project.

It is common practice to model heat transfer problems using an electrical resistance analogy, and it is well known that the resistance R_{12} to heat transfer by radiation between two arbitrary surfaces 1 and 2 is

$$R_{12} = \frac{1-\varepsilon_1}{A_1\varepsilon_1} + \frac{1}{A_2F_{21}} + \frac{1-\varepsilon_2}{A_2\varepsilon_2}, \tag{1}$$

where A is the surface area, ε the surface emissivity, and F a configuration factor. For a cryogenic pipe (subscript p) inside of a vacuum shell (subscript s), with n_s layers of insulation (subscript i) having surface area A_s applied on the shell and n_p layers of area A_p applied on the pipe, resistances between each surface may be added in series to produce, after some basic algebraic rearrangement, an expression for the total resistance R_{sp} between the shell and pipe:

$$R_{sp} = \frac{1-\varepsilon_s}{A_s\varepsilon_s} + \frac{n_s}{A_s}\left(\frac{2-\varepsilon_i}{\varepsilon_i}\right) + \frac{1}{A_pF_{ps}} + \frac{n_p}{A_p}\left(\frac{2-\varepsilon_i}{\varepsilon_i}\right) + \frac{1-\varepsilon_p}{A_p\varepsilon_p}. \tag{2}$$

The first, third, and fifth term are easily recognizable as the resistance to radiation between the shell and pipe as given in (1). The configuration factor $F_{ps} = 1$ since the pipe is entirely contained within the shell. The second and fourth terms are contributions due to MLI on the shell and pipe, respectively. Taking the ratio of pipe to shell insulation resistance (i.e., term four to term two) gives $A_R n_p/n_s$, where $A_R = A_s/A_p$ is the shell to pipe surface area ratio, indicating that just one layer of pipe insulation achieves the same impedance to radiation as A_R layers of shell insulation.

One justification for insulating the vacuum shell anyway might be to reduce its effective emissivity. Isolating the first, third, and fifth terms of (1), and taking the surface of the pipe as a unit area so that $A_R = A_s$, gives a resistance to radiative exchage between the innermost layer of insulation on the shell and the outermost layer on the pipe of $R'_{sp} = (1-\varepsilon_s)/A_R\varepsilon_s + 1/\varepsilon_p$. As the surface area ratio grows, $\lim_{A_R\to\infty} R'_{sp} = 1/\varepsilon_p$, and the dependency on ε_s is eliminated. Treating the shell as a black body radiator ($\varepsilon_s = 1$) yields the same result, indicating that relatively larger shells mimic black body behavior regardless of their actual emissivity. As seen in the left panel of Figure 4, even moderate values of A_R such as may be seen in a refrigerator cold box lower R'_{sp} to very nearly its black body value.

In order to provide the most effective and economical insulation solution, MLI will be applied only to the pipes inside of the SNS 2.1 K cold box, and the shell will be left bare. More detailed analysis including effects of layer to layer conduction will be explored in the detailed design phase.

IOP Conf. Series: Materials Science and Engineering **1344** (2026) 012083 doi:10.1088/1757-899X/1344/1/012083

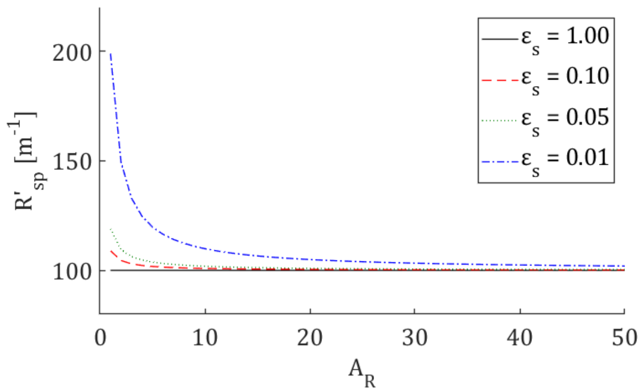

Figure 4. Resistance to radiation heat transfer between two surfaces as a function of the surface area ratio and emissivity of the outer surface (inner surface emissivity $\varepsilon_p = 0.01$ for all cases).

6. Control System Integration

The control system architecture, depicted in Figure 5, follows the general format used on other recent sub-atmospheric cold box projects.

Variable frequency drives (VFDs) housed in separate motor control cabinets (MCCs), powered by a 3-phase, 480 V, 60 Hz source, manage speed control of the cold compressor motors as well as power the AMBs. Regenerative energy conversion obtained from the spinning down compressor wheels powers the AMBs during power failure (battery backup is not necessary).

The Experimental Physics and Industrial Control System (EPICS) open-source software suite is used to create the human machine interface (HMI) and support input/output controller (IOC) configuration for communication between programmable logic controllers (PLCs) and client/server applications. EPICS servers also house database files containing IOC records and variable tags as well as the extensible display manager (EDM) screen creation toolset. From these screens, information may be read or written to the control PLCs through Ethernet protocol.

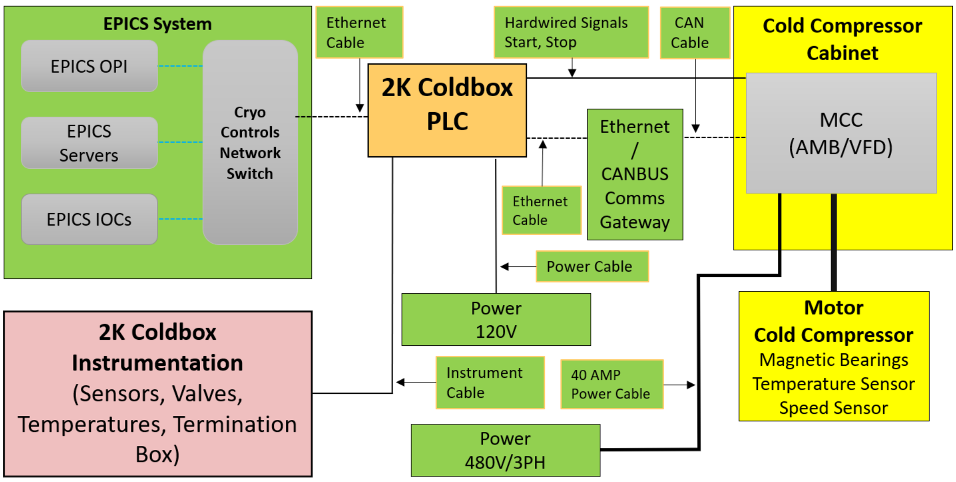

Figure 5. Overview of the control system.

Cold compressor speeds will be adjusted to maintain a constant helium mass flow rate, and electric heaters in the SCL liquid helium baths will regulate the vapor pressure. Proportional-integral-derivative (PID) algorithms coded and processed within the PLCs are responsible for controlling the VFDs and heaters, as well as the remotely operated valves within the cold box, through a closed loop feedback system. The PID settings can be manipulated and adjusted through the EDM screens in the EPICS layer to meet the specific requirements of each process.

The MCCs communicate using the controller area network (CAN) bus protocol, and exchange data, such as compressor speed and motor temperature, with the PLC through an Ethernet/CAN bus gateway converter. Instrumentation for the 2.1 K cold box consists of pressure transducers and temperature diodes installed inside of the cold box and linked to external cabling via feedthrough connector ports built into the vacuum shell. Information from the pressure transducers is received at the PLC as analog input 4-20 mA signals, while signal conditioners are responsible for communicating temperature data from the diodes to the PLC through a predefined voltage curve. These temperature diode conditioners transmit data using Profibus protocol format, communicating with the PLC through Profibus/Ethernet gateways.

7. Conclusions

Conceptually, the replacement 2.1 K cold box for the CHL at SNS will house five cold compressors which can be serviced or replaced without breaking insulating vacuum or disturbing 4.5 K operation of the SCL. Interconnecting piping is sized for turnover time constants of at least 0.5 s and minimal pressure loss, and contains swirl eliminating flow straighteners at each cold compressor inlet. A 10 ft. diameter by 13 ft. high vacuum shell with torispherical heads and all required utility piping is constructed around the cold components. Actively cooled shielding, heat intercepts, and shell-mounted insulation blankets will not be used, since all represent cost and complexity that do not benefit the SNS use case. The control system relies on a proven architecture to integrate cold compressor MCCs, instrumentation, and valving into the existing EPICs system.

Acknowledgments

This work is funded by Oak Ridge National Laboratory, managed by UT-Battelle, LLC, for the US Department of Energy under contract DE-AC05-00OR22725. It was conducted at Jefferson Lab which is supported by the U.S. Department of Energy, Office of Science, Office of Nuclear Physics under contract DE-AC05-06OR23177.

References

[1] Arenius D, Chronis W, Creel J, Dixon K, Ganni V and Knudsen P 2004 *AIP Conf. Proc.* **710** 200
[2] Hatfield D *et al.* 2006 *AIP Conf. Proc.* **823** 1436
[3] Knudsen P, Ganni V, Casagrande F, Fila A, Hasan N, Vargas G and Joseph N 2020 *IOP Conf. Ser.: Mater. Sci. Eng.* **755** 012092
[4] Yang S *et al.* 2020 *IOP Conf. Ser.: Mater. Sci. Eng.* **755** 012120
[5] Casagrande F, Gurd P A, Hatfield D R, Howell M P, Strong W H, Arenius D, Creel J, Ganni V and Knudsen P 2006 *10th European Particle Accelerator Conference (EPAC 06)*
[6] Mastracci B, Yang S, Creel J, Dixon K, Norton R, Thompson S, Wieliczko J and Wijeratne T 2022 *IOP Conf. Ser.: Mater. Sci. Eng.* **1240** 012069
[7] Ganni V, Arenius D M, Bevins B S, Chronis W C, Creel J D and Wilson J D 2002 *AIP Conf. Proc.* **613** 288
[8] Miller R W 1989 *Flow Measurement Engineering Handbook* 2nd edn (New York: McGraw-Hill)
[9] Yang S, Dixon K, Laverdure N, Rath D, Bevins M, Bai H, Kaminski S and Ravindranath V 2017 *IOP Conf. Ser.: Mater. Sci. Eng.* **278** 012091